Journal of Environment & Biotechnology Research
VINANIE PUBLISHERS
www.vinanie.com/jebr

Removal of Cu^{2+} from aqueous solution by adsorption onto quail eggshell: Kinetic and isothermal studies

Akinhanmi Temilade Fola, Adeogun Abideen Idowu,* Adegbuyi Adetutu

Chemistry Department, Federal University of Agriculture, Abeokuta, Nigeria

ORIGINAL RESEARCH ARTICLE

ABSTRACT

Adsorbent prepared from quail eggshell was used for the removal of Cu^{2+} from aqueous solution. The surface morphology of the adsorbent was characterised using scanning electron microscopy (SEM), Fourier transform infrared (FTIR) and X-ray diffraction (XRD). Experimental data obtained from batch equilibrium studies were subjected to two-parameter (Freundlich, Langmuir, Tempkin and Dubinin-Radushkevich (D-R)) and three-parameter (Redlich-Peterson, Sips, Hill and Khan) isotherm models. The experimental data were best fitted to all of the isotherms with correlation coefficient > 0.9. The adsorption energy (E) from the D-R isotherm was found to be 0.08 kJ/mol, which is an indication of physisorption favoured processes. Kinetic data were analysed with pseudo first-order, pseudo second-order, Avrami and Elovich kinetic models. The pseudo first-order and Avrami models best fitted the experimental data with correlation coefficent above 0.99 with an average relative and hybrid errors less than 5%. Intraparticle diffusion model analysis showed that the adsorption process comprises of two stages (rapid and slow phases).

KEYWORDS
adsorption; equilibrium; isotherms; kinetics; quail eggshell

1. INTRODUCTION

The presence of heavy metals in aquatic environment is a major threat to the environment. This is due to their toxic effects on the plants, animals and human health. Discharge of effluents from industrial activities such as electroplating, mining, electrical and electronics, iron and steel production pharmaceuticals, pesticides, organic chemicals, rubber and plastics, etc. are major sources of the heavy metal contamination in the environment, especially copper.

Accumulation of copper in plants results to metabolic disturbances and growth inhibition (Fernandes and Henriques, 1991; Hajiboland and Hasani, 2007). Presence of copper in high concentration cause damage to marine life, destroys vital organs in fishes and also change their sexual behaviour (Ajmal et al., 1998; Munagapati et al., 2010). Various symptoms such as itching, dermatization and keratinisation of the hands and soles of feet have been attributed to copper poisoning in man (Huang et al., 2007). Large dosage exposure to copper is responsible for severe damage in gastro-intestinal, liver and kidneys (Ajmal et al., 1998) while inhalation of copper spray increases the risk of lung cancer among the exposed workers (Aydin et al., 2008). High level of copper compounds in the body may lead to aging, schizophrenia, mental illness, Indian childhood cirrhosis and Wilson's and Alzheimer's diseases (Brewer, 2007; Faller, 2009; Haureau and Faller 2009). Copper has also been implicated in the damage to lipids and DNA (Brewer, 2010). According to the World Health Organisation (WHO, 1998) and United State Environmental Protection Agency (USEPA), the maximum permissible limit of copper in drinking water is 1.3 mg/L (Bajpai and Jain (2010)). It is therefore important to reduce the concentration of copper in industrial effluent to acceptable level before it is discharged into stream or other receiving water bodies.

Corresponding author: **A.A. Idowu**
Tel: +23480306126987
Fax: +23480306126987
E. mail: abuaisha2k3@yahoo.com

Received: 01-06-2016
Revised: 23-08-2016
Accepted: 09-09-2016
Available online: 01-10-2016

Removal of toxic heavy metals from industrial wastewater has been practiced for several decades by the conventional physico-chemical removal methods, such as chemical precipitation, electroplating, membrane separation, evaporation and resin ionic exchange (Matlock et al., 2002; Mohammadi et al., 2005). However, these methods are usually found to be inefficient and expensive, especially when treating wastewater with low concentration of heavy metals (El-Ashtoukhy et al., 2008). Adsorption processes have been reported to be the low-cost promising alternatives for the treatment of heavy metals present in wastewater because it has some obvious advantages (Kratochvil and Volesky, 1998) such as; high efficiency and selectivity for absorbing metals in low concentrations, less energy requirement, broad operational range of pH and temperature, easy reclamation of metals, and easy recycling of the adsorbent. In recent years, many agricultural wastes had been utilized as adsorbent for heavy metal remediation, the list of which is presented in a recent review (Titi and Bello, 2015).

In this study, quail eggshell (a poultry waste) was used for the preparation of adsorbent for the removal of Cu^{2+} from aqueous solution in a batch process. The effect of solution pH, adsorbent dose, initial metal ion concentrations and contact time were investigated. The equilibrium parameters were analyzed with two-parameter (Freundlich, Langmuir, Tempkin and Dubinin-Radushkevich (D-R)) and three-parameter (Redlich-Peterson (R-P), Sips, Hill and Khan) isotherm models. Kinetic data were analyzed with pseudo first-order, pseudo second-order, Avrami, Elovich and Intraparticle diffusion kinetic models.

2. MATERIALS AND METHODS

2.1. Preparation of Cu^{2+} solution

Aqueous solutions of Cu^{2+} at different concentrations were prepared from copper nitrate ($Cu(NO_3)_2$) obtained from British Drug House, London. This was used as adsorbate and was not purified prior to use. Double distilled-deionised water was employed for the preparation of all the solutions and reagents.

2.2. Preparation of adsorbent

Quail eggs were purchased from P.W Feed Poultry, Abeokuta, Nigeria. The eggs were cracked and shells carefully removed after which they were rinsed with distilled water and then oven dried at a temperature of 70 °C for 24 h. The dried eggshell with membrane was grounded and sieved with a mesh of particle size < 0.125 mm and stored in air tight container for future use.

2.3. Characterization and analytical procedure

X-ray diffraction (XRD) data were collected using a PAN Analytical X'Pert PRO X-ray diffractometer with Cu Kα radiation (λ = 1.5418Å). Fourier transform infrared (FT-IR) spectra were recorded from 400 to 4000 cm^{-1} in TENSOR 27 spectrometer (Bruker, Germany) using KBr pellet technique. Surface morphology of the material was analysed using scanning electron microscopy (SEM/EDAX) [VEGA3 TESCAN]. The concentrations of Cu^{2+} in the solutions before and after adsorption were determined using an atomic absorption spectrophotometer (Buck Scientific model 200 VGP). The samples were filtered prior to analysis in order to minimize interference of the adsorbent with the analysis. Non-linear regression analysis method was used for the least square fit data into all the models as explained in previous studies (Adeogun and Balakrishnan, 2015; Adeogun et al., 2016).

2.4. Batch equilibrium studies

Precisely 100 mL of aqueous solutions comprising known Cu^{2+} concentration with predetermined quantity of adsorbent were placed in Erlenmeyer flasks in an orbital shaker. The effects of adsorbent dosage, initial metal concentration and pH on the removal of Cu^{2+} were studied. Sample solutions were withdrawn at intervals to determine the residual Cu^{2+} concentration using atomic absorption spectrophotometer (Buck Scientific model 200 VGP). The amount of Cu^{2+} removed at equilibrium, Q_e (mg/g), was calculated using below equation:

$$Q_e = \frac{(C_o - C_e)V}{W} \quad (1)$$

where C_o (mg/L) is the initial concentration and C_e (mg/L) is the concentration of the Cu^{2+} at equilibrium in the liquid-phase. V is the volume of the solution (L) while W is the mass of the adsorbent.

2.5. Effect of adsorbent dosage

The study on effect of adsorbent dosages on the removal of Cu^{2+} from aqueous solution was carried out at different adsorbent doses ranging between 0.1 – 1.0 g using 100 mg/L of the Cu^{2+} solution. The Erlenmeyer

flasks containing the Cu^{2+} solutions of the same initial concentration but different adsorbent mass were placed on orbital shaker at 200 rpm. After equilibrium attainment, the samples were filtered off and the solution was analyzed for the residual Cu^{2+}.

2.6. Effects of initial Cu^{2+} concentration and contact time

The effects of initial Cu^{2+} concentration and contact time on adsorption process were investigated with 100 ml Cu^{2+} solution of initial concentrations between 50 and 300 mg/L in series of Erlenmeyer flasks with fixed amount of adsorbent (0.8 g) on orbital shaker at 200 rpm. Samples were withdrawn, filtered off and the solution analyzed for the residual Cu^{2+} from the aqueous at preset time intervals.

2.7. Effect of pH on adsorption process

To investigate the effect pH on the adsorption process, series of experiments were carried out on solutions with initial pH varied between 2 and 8. The pH was adjusted with 0.1 M NaOH or 0.1 M HCl and measured using pH meter. The concentration of the solutions, adsorbent dosage and temperature were held constant at 100 mg/L, 0.8 g and 30 ^{o}C respectively.

2.8.Adsorption isotherms

The equilibrium data from this study were described with eight adsorption isotherm models (i.e. 4 each of two-parameter and three-parameter isotherm models). The two-parameter models used were the Langmuir (Langmuir, 1918), Freundlich (Freundlich, 1906), Tempkin (Tempkin and Pyzhev, 1940), Dubinin and Radushkevich (Dubinin and Radushkevich, 1947), while the Redlich and Peterson (Redlich and Peterson, 1959), Sips (Sips, 1948), Hill (Hill, 1949) and Khan (Khan et al., 1997) are the three-parameter isotherm models.

2.9.Biosorption kinetics studies

The procedures for the kinetics studies were basically identical to those of equilibrium tests. The aqueous samples were taken at preset time intervals, and the concentrations of the Cu^{2+} were similarly determined. The amount of metal ion removed at time t, Q_t (mg/g), was calculated using Equation 2,

$$Q_t = \frac{(C_o - C_t)V}{W} \quad (2)$$

where C_o (mg/L) is the initial concentration and C_t (mg/L) is the concentration of Cu^{2+} at time t in the liquid-phase. V is the volume of the solution (L), and W is the mass of the adsorbent.

In order to investigate the mechanisms of the adsorption process, pseudo-first order (Ho and McKay, 1999), pseudo-second-order (Ho and McKay, 1998), Avrami (Avrami, 1940) and Elovich (Zeldowitsch 1934) models respectively were applied to describe the kinetics of biosorption of Cu^{2+} during the process. Due to the fact that the diffusion mechanism cannot be obtained from the kinetics model, the intraparticle diffusion model (Lin et al., 2011) was also tested. A model is adjudged as best-fit and selected based on statistical parameters.

2.10. Statistical test for the kinetics data

The acceptability and hence the best fit model for the kinetic data were based on the square of the correlation coefficients R^2 and the percentage error function which measures the differences (% SSE) in the amount of the metal ion concentration adsorbed at equilibrium predicted by the models, (Q_{cal}) and the experimental value (Q_{exp}). The validity of each model was determined by the average relative error (SSE, %) and hybrid error analysis, which can be expressed as:

$$\%SSE = \frac{100}{N}\sqrt{((Q_{(\exp)} - Q_{(cal)})/Q_{\exp})^2} \quad (3)$$

$$\%HYBRID = \frac{100}{N-P}\sqrt{((Q_{(\exp)} - Q_{(cal)})/Q_{\exp})^2} \quad (4)$$

where N is the number of data points and P is the number of the parameters in the kinetic equation. To confirm the suitability of model for the experimental data, higher R^2 and the lower error values were considered.

3. RESULTS AND DISCUSSION

3.1. Characterization of the adsorbent

SEM micrograph of the eggshell is shown in Figure 1, it was clear that the powder layer exhibited a porous microstructure with micro-pores which were relatively well separated and homogeneously distributed over the surface. From this image it was certain that

the adsorbent is porous with vast surface and fibril structure which is responsible for its good adsorption capacity.

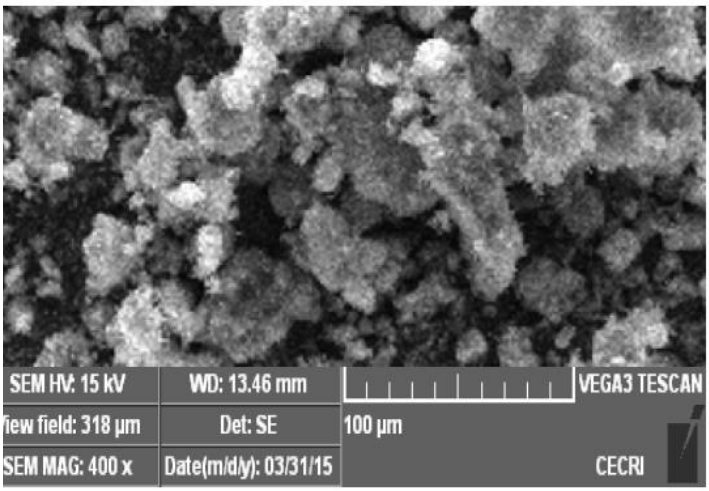

Figure 1. SEM Analysis of quail eggshell

The XRD analysis revealed the crystal structure of eggshell and the diffraction pattern is shown in Figure 2. Eight characteristic peaks were displayed by the diffraction pattern at $2\theta = 29.7°$ (main peak), 36.3°, 39.8°, 43.6°, 47.9°, 48.9°, 57.8°, and 65.8°, which corroborates the presence of calcite ($CaCO_3$) in various forms in the structure of eggshell.

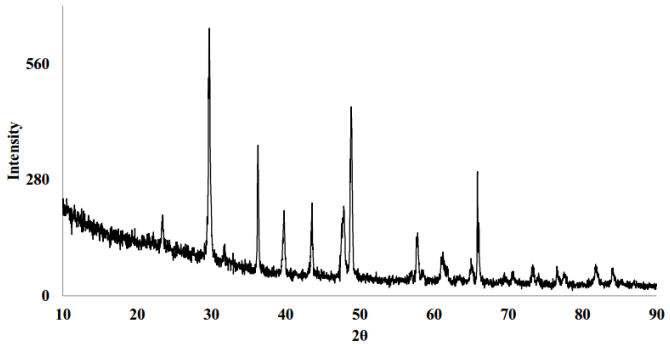

Figure 2. XRD Analysis of quail eggshell

Adsorption on the surface of adsorbent is partly dependent on the functional groups present on such surface, their quantity and affinity for the adsorbate. The presence of functional groups on the surface of adsorbents was confirmed before and after adsorption using FTIR analysis as shown in Figure 3. Figure 3a shows characteristic peaks at 3872 and 3455cm^{-1} which could be attributed to –CONH– and C=O. The most intense peak at 1422 cm^{-1} is attributed to carbonate minerals presents in the egg shell, while those at 875 and 709 cm^{-1} belongs to C–N, N–H, and C–C vibrations (Tsai et al., 2006). Upon adsorption of Cu^{2+} the peak at 3872 cm^{-1} disappeared, while others have undergone a slight shift from their initial positions (Figure 3b).

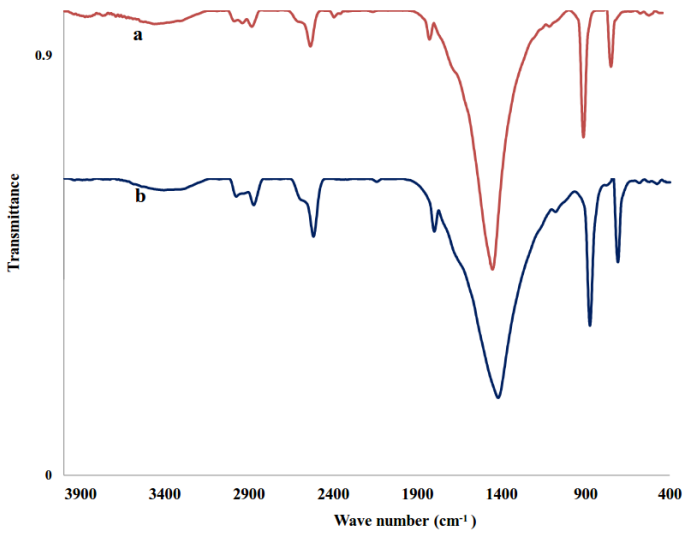

Figure 3. FTIR spectrum of the adsorbent (a) before and (b) after adsorption

3.2. Effect of pH on biosorption process

The solution pH has significant effects on the surface functional groups of the adsorbent as well as the Cu^{2+} species present in the solution, hence pH is one of the most influencing parameters in the biosorption process. The effect of pH on the percentage of Cu^{2+} adsorbed is shown in Figure 4. The adsorption capacity increases as the pH of the solution is increased from 2 to 7. The lower removal efficiency at low pH may be ascribed to competition of metal ions species and H+ for the available sites. As the pH increases from 2 to 7 competitions for the biosorption sites reduced and more Cu^{2+} were removed from the solution. As the solution approaches basic pH, precipitation of the metal ion may be responsible for the decrease in the percentage metal ion removed (Vukovic et al., 2011).

3.3. Effect of adsorbent dosage

The plot of adsorbent dosage against the efficiency of Cu^{2+} removal is shown in Figure 5. It was observed that as the quantity of the adsorbent increased from 0.1 to 0.2 g, the removal efficiency increased from 58 to 91 % as a result of increase in total adsorbent surface area and adsorption sites. Further increase in the adsorbent dosage resulted in reduced efficiency

which could be attributed to the particle interactions, such as aggregation, resulting from high adsorbent concentrations which lead to a reduction of the active surface area of the adsorbent (Kakavandi et al., 2015).

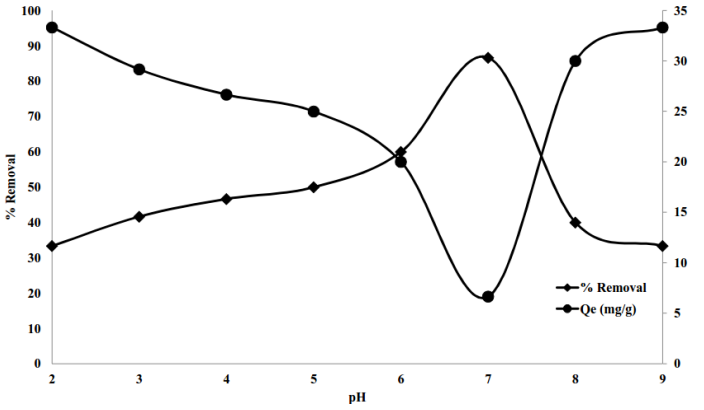

Figure 4. Effect of pH on removal of Cu^{2+} from aqueous solution. Condition: adsorbent dosage = 0.8 g, [Cu^{2+}] = 100 mg/L, temperature = 30 °C.

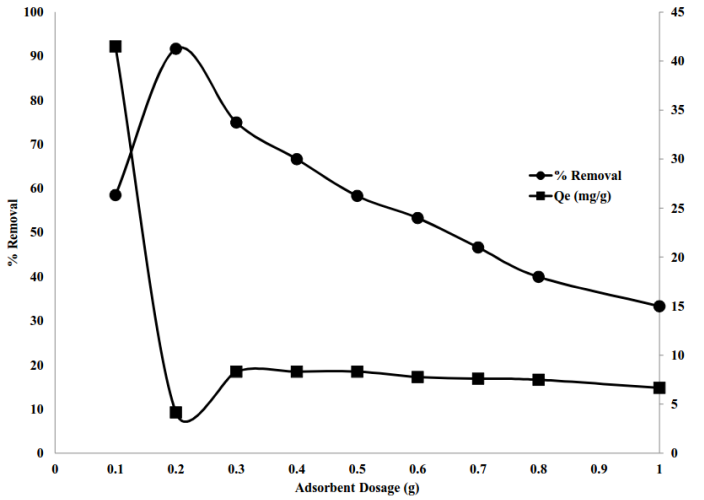

Figure 5. Effect of adsorbent dosage on removal of Cu^{2+} from aqeous solution. Condition: pH 7, [Cu^{2+}] = 100 mg/L, temperature = 30 °C.

3.4. Effect of initial Cu^{2+} concentration

The effect of initial metal ion concentration on the adsorption process is shown in Figure 6. The process showed a rapid removal in the first 30 min, with increased efficiency from 18.6 to 90.4 mg/g as the initial concentration of Cu^{2+} increase from 50 to 300 mg/L. The observed increase in the adsorption capacity as the concentration increases may be due to the increased driving force of the concentration gradient. As there is no significant difference in the quantity of the Cu^{2+} after 120 min of the process, a steady-state approximation was assumed and a quasi-equilibrium situation was reached.

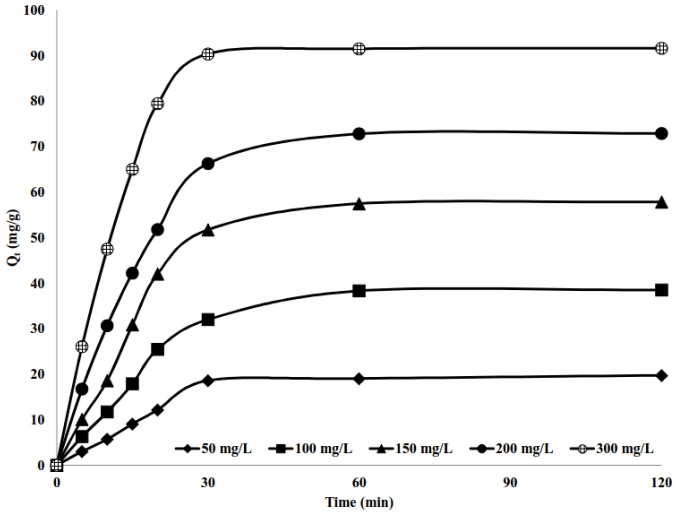

Figure 6. Effect of initial concentration on removal of Cu^{2+} from aqueous solution. Condition: Biosorbent dosage = 0.8 g, pH = 7, temperature = 30 °C.

3.5. Adsorption isotherms

The adsorption equilibrium data obtained at different initial Cu^{2+} concentrations were described using eight different isotherm models. The equation representing these models and the parameters are summarized in Table 1, the detail of which have been explained elsewhere (Foo and Hameed, 2010; Adeogun and Balakrishnan, 2015; Adeogun et al., 2016).

The acceptability and suitability of the isotherm equation to the equilibrium data were based on the values of the correlation coefficients (R^2) estimated from linear regression of the least square fit statistic on Micro Math Scientist software.

Figure 7 represents the adsorption isotherms for (a) two parameter models and (b) three parameter models, the parameters for these isotherm fit are presented in Table 2. The adsorption data fitted well with Langmuir (two-parameter), Sips and Hill (three-parameter) isotherms with highest R^2 (Table 2). The n value > 1 from Freundlich and maximum adsorption capacity of 134.21 mg/g from Langmuir with R_L < 1 obtained are the indication that the adsorption is favorable on the investigated adsorbent. The mean biosorption energy E obtained from Dubinin–Radushkevich was 0.08 kJ/mol, which is an indication of physisorption dominated processes, similar observation had been reported in the literature (Veli and Alyüz, 2007).

Table 1. Isotherm models used for the study of the adsorption of Cu^{2+} on quail eggshell.

Isotherm name	Isotherm model	Parameters
Langmuir	$Q_e = \frac{Q_{max} b C_e}{1 + b C_e}$	Q_{max} and b
Freudlinch	$Q_e = K_F C_e^{1/n}$	K_F and n,
Temkin	$Q_e = \frac{RT}{B_T} \ln(A_T C_e)$	
Dubinin–Radushkevich	$Q_e = Q_s Exp\left(-\frac{\left(RT \ln\left(1+\frac{1}{C_e}\right)\right)^2}{2E^2}\right)$	Q_s and E
Redlich–Peterson	$Q_e = \frac{Q_o C_e}{(1 + K_R C_e^{\ g})}$	Q_o, K_R and g
Sip	$Q_e = \frac{Q_s (K_s C_e)^{\beta_s}}{(1 + (K_s C_e)^{\beta_s})}$	Q_s, K_s and β_s
Hill	$Q_e = \frac{Q_H C_e^{\ n_H}}{(K_H + C_e^{\ n_H})}$	Q_H, K_H and n_H
Khan	$Q_e = \frac{Q_k B_k C_e}{(1 + B_k C_e)^{A_k}}$	Q_k, A_k and B_k

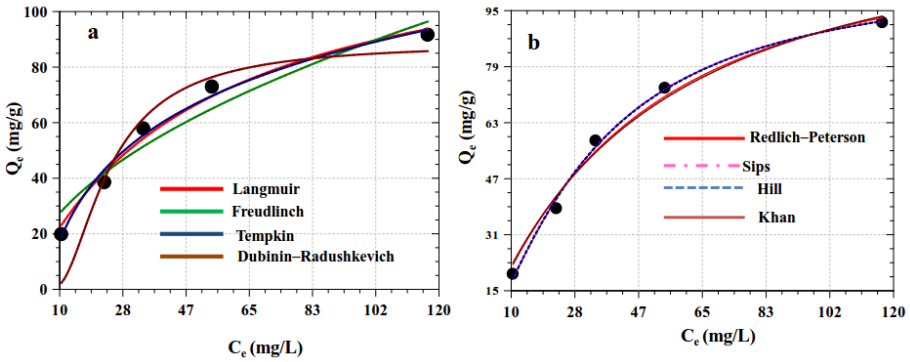

Figure 7. Isothermal fits for the adsorption process, (a) two-parameter and (b) three-parameter fit

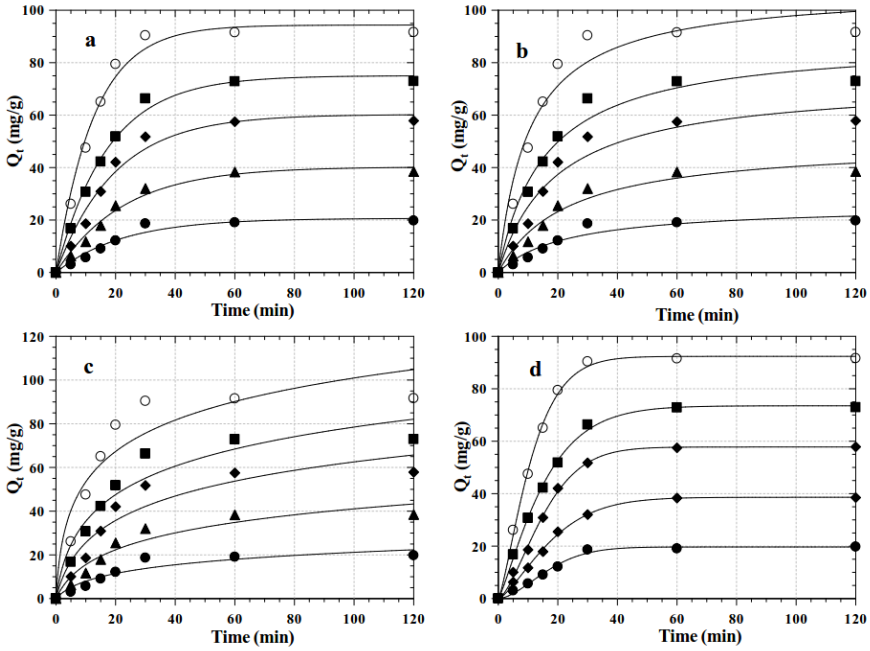

Figure 8. Kinetic fits for the adsorption process, (a) pseudo first-order (b) pseudo second order (c) Elovich and (d) Avrami kinetic models.

Table 2. Isotherm parameters for the adsorption of Cu^{2+} on quail eggshell

Isotherm	Parameters	Values
Langmuir	Q_{max} (mg/g)	134.21
	b (L/mg)	0.02
	R_L	0.29
	R^2	0.997
Freudlinch	K_F (mg/g (mg/L)$^{-1/n}$)	8.40
	n	1.95
	R^2	0.989
Tempkin	A_T (L/g)	0.18
	B_T (J/mol g mg)	80.04
	R^2	0.998
Dubinin–Radushkevich	Q_s (mg/g)	88.54
	E (kJ/mol)	0.08
	R^2	0.981
Redlich–Peterson	Q_0 (mg/g)	2.44
	K_R (mg/g)$^{1/g}$	0.01
	g	1.12
	R^2	0.998
Sips	Q_s (mg/g)	106.08
	K_s (mg/L)$^{1/\beta_s}$	0.03
	β_s	1.43
	R^2	0.999
Hill	Q_H (mg/g)	107.00
	K_H (mg/L)$^{1/n_H}$	129.13
	n_H	1.40
	R^2	0.999
Khan	Q_k (mg/g)	155.84
	A_k	1.09
	B_k (mg/L)	0.02
	R^2	0.998

Table 3. Kinetic models for the adsorption of Cu^{2+} on quail eggshell.

	Kinetic model	Parameters
Pseudo First Order	$Q_t = Q_e(1 - e^{(-k_1 t)})$	Q_e and k_1
Pseudo Second Order	$Q_t = \frac{Q_e^2 k_2 t}{(1 + Q_e k_2 t)}$	Q_e and k_2
Elovich	$Q_t = \frac{1}{\beta}\ln(\alpha\beta t)$	α and β
Avramin	$Q_t = Q_e(1 - e^{(-k_{av} t^{n_{av}})})$	k_{av}, *and* n_{av}
Intraparticle model	$Q_t = K_{id} t^{0.5} + C_i$	K_{id} and C_i

3.6. Kinetics of biosorption

The plots of four different kinetic models used to explain the adsorption data are shown in Figure 8 (a – d). The equations for these models are shown in Table 3, details of which have explained elsewhere (Adeogun et al., 2011; Lin et al., 2011; Ahmad et al., 2014; Adeogun and Balakrishnan, 2015).

Upon analyzing the kinetic parameters as shown in Table 4, Avramin kinetic model best fitted the kinetic data with n values 1.2 and 1.7 suggesting nucleation of the metal ion on the adsorbent. The rate constant increases with increase in initial Cu^{2+} concentration; this shows that at higher initial concentration the electrostatic interaction increased at the site, thereby increasing the adsorption rate. The behaviour of Elovich constant shows that the process of biosorption comprises of more than one mechanism.

3.7. Adsorption mechanism

The mechanism of biosorption was investigated by subjecting the data to intraparticle diffusion model. The plot is shown in Figure 9 which reveals the existence of two successive adsorption steps. The first stage was faster than the second, and it can be attributed to the external surface adsorption referred to as the boundary layer diffusion. Thereafter, the second linear part can be attributed to the intraparticle diffusion stage; this stage is the rate controlling step. Table 5 shows the intraparticle model constants for the adsorption of Cu^{2+} on quail eggshell. The K_{di} values were found to increase with concentration. The increase in Cu^{2+} concentration results in an increase in the driving force

Table 4. Kinetic parameters for the adsorption of Cu^{2+} on quail eggshell

		Kinetic parameters				
	C_o (mg/L)	50 mg/L	100 mg/L	150 mg/L	200 mg/L	300 mg/L
	C_e (mg/L)	10.50	23.00	34.31	54.21	116.78
	Q_{exp} (mg/g)	19.75	38.50	57.84	72.89	91.61
Pseudo First-order	Qe (mg/g)	20.67	40.26	60.26	75.04	94.35
	$k_1 x10^{-2}$ (min^{-1})	4.49	4.43	5.09	5.76	7.84
	R_2	0.987	0.995	0.993	0.998	0.998
	ΔQe_{SSE}	0.58	0.57	0.52	0.37	0.37
	ΔQe_{HYBRID}	0.66	0.65	0.60	0.42	0.43
Pseudo Second-order	Qe (mg/g)	25.58	49.66	73.00	88.77	108.14
	k_2 $x10^{-4}$(g/mg min)	17.1	8.82	7.19	7.20	8.91
	R^2	0.980	0.989	0.986	0.993	0.991
	ΔQe_{SSE}	3.69	3.62	3.28	2.72	2.26
	ΔQe_{HYBRID}	4.22	4.14	3.74	3.11	2.58
Elovich	α (mg/(g min))	1.54	3.02	5.68	9.62	23.97
	β (g/mg)	0.15	0.08	0.06	0.05	0.05
	$Q_{e\,t=0}$ (mg/g)	6.65	12.83	17.93	20.21	21.34
	R^2	0.969	0.980	0.976	0.984	0.979
	ΔQe_{SSE}	1.74	0.65	3.35	5.65	8.54
	ΔQe_{HYBRID}	1.99	0.74	3.83	6.45	9.76
Avramin	Qe (mg/g)	19.67	38.62	57.79	73.50	92.34
	$k_1 x10^{-2}$ (min^{-1})$^{n}_{av}$	0.67	1.52	1.30	3.31	3.68
	n_{av}	1.70	1.40	1.52	1.22	1.31
	R^2	0.997	0.999	0.999	0.999	0.999
	ΔQe_{SSE}	0.05	0.04	0.01	0.10	0.10
	ΔQe_{HYBRID}	0.06	0.04	0.01	0.12	0.11

thereby increasing the diffusion rate. The mechanism of adsorption is best described as microprecipitation of Cu^{2+} on the surface of adsorbent as a result of presence of $CaCO_3$ which is in agreement with observations of Vijayaraghavan et al. (2005) and Vijayaraghavan and Joshi (2013).

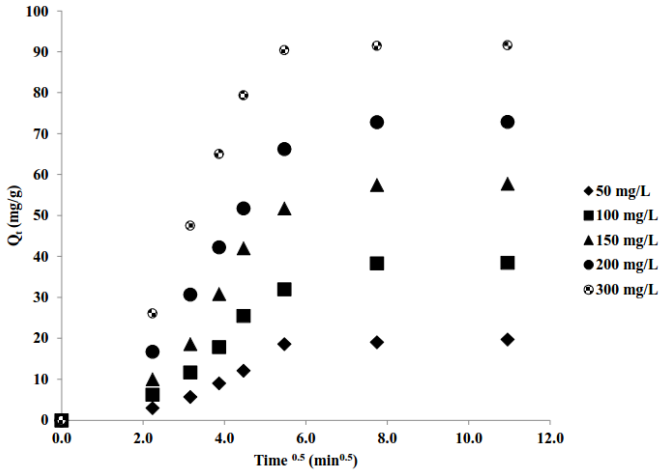

Figure 9. Intraparticle diffusion fit for the adsorption process.

Table 5. Intraparticle diffusion parameters for adsorption of Cu^{2+} on quail eggshell

	Intraparticle diffusion parameters				
C_o (mg/L)	50 mg/L	100 mg/L	150 mg/L	200 mg/L	250 mg/L
K_{1d} (mg/g $min^{0.5}$)	2.61	5.37	8.98	11.52	17.70
C_1(mg/g)	1.19	2.49	4.35	3.37	5.02
R^2	0.968	0.964	0.962	0.989	0.990
K_{2d} (mg/g $min^{0.5}$)	0.88	1.85	2.12	2.74	1.40
C_2(mg/g)	11.06	20.33	37.10	46.34	78.19
R^2	0.986	0.994	0.995	0.994	0.998

4. CONCLUSIONS

The result of this study revealed the capability of using quail eggshell, a poultry waste for remediation of Cu^{2+} contaminated wastewater through adsorption processes. The adsorption efficiency was optimum at pH 7 and 0.2 g/L adsorbent dosage. The maximum adsorption capacity was 134.21 mg/g. The kinetics of the process was best explained using Avrami kinetics model, with high $R^2 > 0.99$. Intraparticle diffusion was not the sole rate controlling factor, microprecipitation of Cu^{2+} on the surface of adsorbent as a result of presence of $CaCO_3$ also affected the adsorption process. Fixed bed adsorption study for large adaptation is highly recommended.

ACKNOWLEDGEMENTS

The financial support in the form of grants from CSIR, for twelve months TWAS-CSIR Postdoctoral Fellowship, FR number: 3240275035, awarded to Abideen Idowu Adeogun that enables part of this work to be carried out is highly acknowledge. Also he is thankful to the authority of the Federal University of Agriculture, Abeokuta, Nigeria for granting the study leave to honour the fellowship.

REFERENCES

Adeogun A.I., Sunday, O. and Olateju, K.S. (2016) Removal of Mn(II) from aqueous solution by *Irvingia gabonensis* immobilized *Aspergillus* sp. TU-GM14 isothermal, kinetics and thermodynamic studies. Journal of Environment and Biotechnology Research, 2, 1-11.

Adeogun, A.I. and Balakrishnan, R.B. (2015) Kinetics, isothermal and thermodynamics studies of electrocoagulation removal of basic dye rhodamine B from aqueous solution using steel electrodes. Applied Water Science, 5, 1-13.

Adeogun A. I. and Balakrishnan R. B. (2015) One-Step synthesized calcium phosphate based material for the removal of Alizarin S dye from aqueous solutions: isothermal, kinetics and thermodynamics studies. Journal of Applied Nanoscience, 5, doi:10.1007/s13204-015-0484-9.

Adeogun A.I., Ofudje, A.E., Idowu, M. and Kareem, S.O. (2011) Equilibrium, kinetic and thermodynamic studies of the biosorption of Mn (II) ions from aqueous solution by raw and acid-treated corncob biomass. Bioresources, 6, 4117-4134.

Ahmad, M. A., Puad, N. A. A and Bello, O. S (2014) Kinetic, equilibrium and thermodynamic studies of synthetic dye removal using pomegranate peel activated carbon prepared by microwave-induced KOH activation. Water Resources and Industry, 6, 18-35.

Ajmal, M., Khan, H., Ahmad, S and Ahmad, A (1998) Role of sawdust in the removal of copper(II) from industrial wastes. Water Research, 32, 3085–3091.

Avrami, M. (1940) Kinetics of phase change. II transformation-time relations for random distribution of nuclei. The Journal of Chemical Physics, 8, 212-224.

Aydin, H., Bulut, Y. and Yerlikaya, C. (2008) Removal of copper(II) from aqueous solution by adsorption onto low-cost adsorbents. Journal of Environmental Management, 87, 37-45.

Bajpai, S. K. and Jain, A (2010) Removal of copper(II) from aqueous solution using spent tea leaves (STL) as a potential sorbent. Water SA, 36, 221-228.

Brewer G. J (2010) Copper toxicity in the general population. Clinical Neurophysiology, 121, 459-460.

Brewer, G. J (2007) Iron and copper toxicity in diseases of aging, particularly atherosclerosis and Alzheimer's disease. Experimental Biology and Medicine, 232, 323-335.

Dubinin, M.M. and Radushkevich, L.V. (1947) Equation of the characteristic curve of activated charcoal, Proceedings of the Academy of Sciences, Physical Chemistry Section, U.S.S.R., 55, 331 – 333.

El-Ashtoukhy, E.S., Amin, N. K. and Abdelwahab, O. (2008). Removal of lead (II) and copper(II) from aqueous solution using pomegranate peel as a new adsorbent. Desalination, 223, 162-173.

Faller, P. (2009) Copper and zinc binding to amyloid-beta coordination, dynamics, aggregation, reactivity and metal-ion transfer. Chembiochem, 10, 2837–2845.

Fernandes, J.C. and Henriques, F.S. (1991) Biochemical, physiological and structural effects of excess copper in plants. Botanical Review, 57, 246–273.

Foo, K.Y. and Hameed, B.H. (2010) Insights into the modeling of adsorption isotherm systems. Chemical Engineering Journal, 156, 2–10.

Freundlich, H.M.F. (1906) Over the adsorption in solution, Journal of Physical Chemistry, 57, 385–471.

Hajiboland, R. and Hasani, B. D. (2007) Effect of Cu and Mn toxicity on chlorophyll fluorescence and gas exchange in rice and sunflower under different light intensities. Journal of Stress Physiology and Biochemistry, 3, 4–17.

Haureau, C. and Faller P. (2009) A beta-mediated ROS production by Cu ions structural insights, mechanisms and relevance to Alzheimer's disease, Biochimie, 91, 1212-1217.

Hill, T.L. (1949) Physical adsorption and the free volume model for liquids. The Journal of Chemical Physics, 17, 590-590.

Ho, Y.S. and McKay, G. (1998) Kinetic models for the sorption of dye from aqueous solution by wood. Process Safety and Environmental Protection, 76, 183-191.

Ho, Y.S and McKay, G. (1999) Pseudo-second order model for sorption processes. Process Biochemistry, 34, 451-465.

Huang, Y.H., Hsueh, C.L., Cheng, H.P., Su, L.C. and Chen, C.Y. (2007) Thermodynamics and kinetics of adsorption of Cu (II) onto waste iron oxide. Journal of Hazardous Materials, 144, 406-411.

Kakavandi, B., Kalantary, R.R., Jafari, A.J., Nasseri, S., Ameri, A., Esrafili, A. and Azari, A. (2015) Pb (II) adsorption onto a magnetic composite of activated carbon and superparamagnetic Fe3O4 nanoparticles: Experimental and modeling study. CLEAN– Soil, Air, Water, 43, 1157-1166.

Khan, A.R. Ataullah, R. and Al-Haddad, A. (1997) Equilibrium adsorption studies of some aromatic pollutants from dilute aqueous solutions on activated carbon at different temperatures. Journal of Colloid and Interface Science, 194, 154–165.

Kratochvil, D. and Volesky, B. (1998) Advances in the biosorption of heavy metals. Trends in Biotechnology, 16, 291-300.

Langmuir, I. (1918) The adsorption of gases on plane surfaces of glass, mica and platinum. Journal of American Chemical Society, 40, 1361-1403.

Lin, J., Zhan, Y. and Zhu, Z. (2011) Adsorption characteristics of copper (II) ions from aqueous solution onto humic acid-immobilized surfactant-modified zeolite. Colloids and Surfaces A: Physicochemical and Engineering Aspects, 384, 9-16.

Matlock, M.M., Howerton, B. and Atwood, D.A. (2002) Chemical precipitation of heavy metals from acid mine drainage. Water Research, 36, 4757–4764.

Mohammadi, T., Mohen, M.S., and Razmi, A. (2005) Modeling of metal ion removal from waste water by electrodialysis. Separation and Purification Technology, 41, 73–82.

Munagapati, V.S. Yarramuthi, V. Nadavala, S.K. Alla, S.R and Abburi, K. (2010) Biosorption of Cu(II), Cd(II) and Pb(II) by *Acacia leucocephala* bark powder: Kinetics, equilibrium and thermodynamics. Chemical Engineering Journal, 157, 357–365.

Redlich, O and Peterson, D.L. (1959) A useful adsorption isotherm, Journal of Physical Chemistry, 63, 1024–1026.

Sips, R (1948) Combined form of Langmuir and Freundlich equations, Journal of Chemical Physics, 16 490–495.

Tempkin, M.I. and Pyzhev, V. (1940) Kinetics of ammonia synthesis on promoted iron catalyst, Acta Physica Chimca. USSR 12 (1940) 327–356.

Titi, O.A. and Bello, O.S. (2015) An overview of low cost adsorbents for copper (II) ions removal. Journal of Biotechnology and Biomaterials, 5, 177.

Veli, S. and Alyüz, B. (2007). Adsorption of copper and zinc from aqueous solutions by using natural clay. Journal of Hazardous Materials, 149, 226-233.

Vijayaraghavan, K. and Joshi, U.M. (2013) Chicken eggshells remove Pb(II) ions from synthetic wastewater, Environmental Engineering Science, 30, 67-73.

Vijayaraghavan, K., Jegan, J., Palanivelu, K. and Velan M. (2005) Removal and recovery of copper from aqueous solution by eggshell in a packed column. Minerals Engineering, 18, 545-547.

Vukovic, G.D., Marinkovic, A.D., Skapin, S.D., Ristic, M.D., Aleksic, R., Peric-Grujic, A.A. and Uskokovic, P.S. (2011) Removal of lead from water by amino modified multi-walled carbon nanotubes. Chemical Engineering Journal, 173, 855-865.

WHO, World Health Organization (1998) Aluminum in guidelines for drinking-water quality, Second Edition, Addendum to Volume 2, Health Criteria and Other Supporting Information Geneva World Health Organization, pp. 3-13.

Zeldowitsch, J. (1934) Über den mechanismus der katalytischen oxidation von CO an MnO_2. Acta Physicochimica URSS, 1, 364 - 449.